
BEYOND LINEARITY AND TIME-HOMOGENEITY: RELATIONAL HYPER EVENT MODELS WITH TIME-VARYING NON-LINEAR EFFECTS

Martina Boschi*

`martina.boschi@usi.ch`
Università della Svizzera italiana
Via la Santa 1, 6962
Lugano-Viganello, Switzerland

Jürgen Lerner

`juergen.lerner@uni-konstanz.de`
University of Konstanz
Konstanz, Germany

Ernst C. Wit

`ernst.jan.camiel.wit@usi.ch`
Università della Svizzera italiana
Lugano, Switzerland

ABSTRACT

Recent technological advances have made it easier to collect large and complex networks of time-stamped relational events connecting two or more entities. Relational hyper-event models (RHEMs) aim to explain the dynamics of these events by modeling the event rate as a function of statistics based on past history and external information.

However, despite the complexity of the data, most current RHEM approaches still rely on a linearity assumption to model this relationship. In this work, we address this limitation by introducing a more flexible model that allows the effects of statistics to vary non-linearly and over time. While time-varying and non-linear effects have been used in relational event modeling, we take this further by modeling joint time-varying and non-linear effects using tensor product smooths.

We validate our methodology on both synthetic and empirical data. In particular, we use RHEMs to study how patterns of scientific collaboration and impact evolve over time. Our approach provides deeper insights into the dynamic factors driving relational hyper-events, allowing us to evaluate potential non-monotonic patterns that cannot be identified using linear models.

Keywords relational hyper event model (RHEM); generalized additive model (GAM); tensor product smooths; time-varying effect; non-linear effect; non-monotonic patterns;

*Corresponding author

List of Abbreviations:

- REM: Relational Event Model
- RHEM: Relational Hyper Event Model
- GAM: Generalized Additive Model
- TVE: Time-Varying Effect
- NLE: Non-Linear Effect
- LE: Linear Effect
- TVNLE: *Joint* Time-Varying Non-Linear Effect
- TPRS: Thin Plate Regression Spline
- TPS: Thin Plate Spline
- GAM: Generalized Additive Model
- MLE: Maximum Likelihood Estimator
- ECDF: Empirical Cumulative Distribution Function
- LogLik: Log-Likelihood

1 Introduction

Activities such as sending e-mails [Perry and Wolfe, 2013, Boschi and Wit, 2024], executing financial transactions [Bianchi and Lomi, 2023], attending meetings [Lerner et al., 2021], citing academic references [Filippi-Mazzola and Wit, 2024b, Lerner et al., 2025], co-participating in criminal activities [Bright et al., 2024], and collaborating in cultural production [Burgdorf et al., 2024] represent distinct social phenomena, that share a fundamental characteristic: they can all be represented as *temporal interactions* involving two or more participants. This relational perspective lies at the heart of social network analysis and distinguishes it from other analytical frameworks [Wasserman, 1994]. In an event-based representation of temporal networks, social dynamics are modeled as collections of time-stamped edges that capture the evolving structure of relationships over time [Lambiotte and Masuda, 2016]. The aforementioned examples often involve relationships that extend beyond simple dyadic interactions, consisting of complex and multi-actor activities occurring at specific points in time. We refer to these richer forms of interaction as *hyperevents* [Lerner et al., 2021] — mathematically represented as time-stamped *hyperedges* [Berge, 1989], i.e., sets of nodes of arbitrary size. Modeling these hyperevents involves accounting for the polyadic nature of such interactions [Seidman, 1981].

An increasing number of studies have focused on describing temporal hypergraphs using temporal motifs and relative counts [Paranjape et al., 2017, Wang et al., 2020, Lee and Shin, 2023]. However, such approaches do not model the dynamics of how hyperedges emerge. Some progress has been made in detecting changes in the dynamics of temporal hypergraphs driven by specific factors [Zou and and, 2017]. Notably, Benson et al. [2018] propose a generative stochastic model that predicts and explains the occurrence of sets of entities — interpretable as hyperevents — based on previously observed subsets. This growing interest in modeling complex, time-stamped group interactions has led to the extension of traditional *Relational Event Models* (REMs), which primarily focus on sequences of events involving a sender and a receiver [Butts, 2008, Bianchi et al., 2024], into the hypergraph domain. *Relational Hyper Event Models* (RHEMs) aim to capture the complex dynamics of polyadic events, conceived as interactions involving multiple participants simultaneously [Lerner et al., 2021, Lerner and Lomi, 2023]. Going beyond the initial proposal by Perry and Wolfe [2013] for modeling *multi-cast interactions*, RHEMs provide a comprehensive framework for understanding the dynamics of social-relational hyper-event processes. Related intensity processes are modeled as functions of higher-order covariates [Lerner and Lomi, 2023]. Recent RHEM formulations allow for the analysis of dependencies among nodes across different network modes, accommodating entities with inherently distinct characteristics — such as authors (scientists) and references (scientific papers) within a publication network [Lerner et al., 2025]. The computational efficiency in calculating hyperedge covariates, enabled by the open-source software *eventnet* [Lerner and Lomi, 2020, 2023], makes RHEMs a practical tool in social network analysis. This facilitates the investigation of dynamic network effects — such as preferential attachment, (partial) repetition, and triadic closure — that may hold theoretical or empirical significance.

Despite significant advancements in the RHEM literature, current formulations remain constrained by a fundamental limitation: they assume linearity in hyperevent effects. This reliance introduces two key drawbacks. First, it overlooks the temporal variability of effects. In temporal networks — where endogenous and complex dynamics are inherently time-dependent — several REM formulations have underscored the importance of incorporating time-varying effects into empirical applications [Bianchi and Lomi, 2023, Juozaitienė et al., 2023, Boschi et al., 2025]. Second, the linearity assumption restricts the flexibility of existing REM frameworks, limiting their capacity to capture how covariate effects vary as a function of their values [Bauer et al., 2022, Filippi-Mazzola and Wit, 2024a, Filippi-Mazzola et al., 2024]. This limitation is particularly relevant when covariates are evaluated in terms of their *internal time* [Juozaitienė and Wit, 2024, Amati et al., 2024], a common scenario for many endogenous covariates in relational event modeling. Mechanisms such as *reciprocity* and *repetition* — computed from previous events in the opposite and same direction respectively — can be more effectively assessed by considering the time intervals between current and past relevant events. While these prior interactions influence the rate of events, their impact typically weakens with time — a phenomenon referred to as *forgetfulness* [Juozaitienė and Wit, 2024]. To capture this decaying influence, it is advantageous to model these covariates, measured as internal times, using non-linear effects. This allows the decay patterns to be learned directly from the data, rather than imposing a rigid, prespecified functional form. Such flexibility is helpful, because relying on an incorrect decay function can lead to erroneous conclusions [Arena et al., 2023]. A related and equally important phenomenon is *saturation*, which arises when individuals face cognitive overload and become unable to effectively process additional information [Atienza-Barthelemy et al., 2025]. Within the RHEM framework, saturation can be modeled by allowing the influence of certain drives on the event rate to exhibit a non-linear pattern — initially increasing with exposure but eventually reaching a plateau or declining.

This paper addresses the primary limitation of current RHEM formulations by incorporating recent advancements from the REM literature, particularly regarding *time-varying effects* (TVE) and *non-linear effects* (NLE). However, our contribution goes beyond a straightforward adaptation of TVE and NLE to the context of relational hyper event modeling. We introduce a novel framework that enables effects to be *jointly time-varying and non-linear*. This is

accomplished through the use of *tensor product bases*, which allow for the construction of smooth functions involving multiple covariates simultaneously [Wood, 2017]. As a result, the proposed method supports the representation of a smooth interaction term, defined on the Cartesian product of time and the covariate of interest.

The primary contribution of this paper is presented in Section 2, which outlines both the modeling framework and the inference techniques for relational hyperevent sequences. Section 3 describes a simulation study using synthetic relational hyperevent data. The results show that when the true data-generating process involves time-varying effects, non-linear effects, or the two of them jointly, the linear model fails to capture these dynamics. In contrast, the proposed model successfully recovers these effects. Moreover, when the assumption of linearity holds, the proposed framework naturally reduces to the correct linear specification, recovering it as a special case. Section 4 presents empirical results on scientific collaboration, extending the models developed by Lerner et al. [2025]³. In this application, we find evidence for effects that are linear and fixed in time, non-linear, and jointly time-varying and non-linear, demonstrating the relevance of this approach in empirical hyperevent applications that take place over a long period — 80 years in our case.

2 Dynamic Hypernetwork Modeling

A *dynamic hypernetwork* is a temporal system in which hyperevents “occur”. These systems are also called *relational hypernetworks*. They are made up of a sequence of *hyperevents*, written as:

$$E = \{(t_m, I_m, J_m)\}, \quad m = 1, \dots, n, \quad (1)$$

where t_m is the time when a group of *senders* I_m interacts with a group of *receivers* J_m . All participants are nodes in a vertex set V of a *temporal hypergraph*. Depending on the context, senders and receivers may belong to the same or different groups. If they belong to the same group, the system is a *one-mode system*. If they play different roles, the system is a *two-mode system*. In the two-mode case, the vertex set V of the *two-mode temporal hypergraph* is divided into two disjoint sets: V^I for possible senders and V^J for possible receivers. If entities join or leave the system over time, these sets can vary with time and are written as V_t^I and V_t^J . In our empirical study, we focus on a two-mode system related to scientific publications, where a group of authors (senders) cite a group of previously published papers (receivers). The notation (t_m, I_m, J_m) in Equation 1 naturally describes *directed hyperevents*, where sender and receiver groups are distinct. However, some interactions do not involve such roles. For example, in a *meeting*, participants interact together at the same time without a sender-receiver distinction. In such cases, we can describe the event as an *undirected hyperevent* by setting $J_m = \emptyset$ and including all participants in I_m . We denote the maximum size allowed for a meeting as w . Mathematically, undirected hyperevents represent *undirected hyperedges*, which are subsets of the vertex set V , while directed hyperevents correspond to *directed hyperedges*.

2.1 Relational Hyperevent Model

The event sequence in Equation (1) is treated as a realization of a *marked point process*. In this process, the *points* represent the times t when hyperevents occur, and the *marks* specify the senders I and receivers J involved in each event. Related to this point process is a *counting process* $N(t, I, J)$, which records the number of hyperevents from group I to group J observed up to time t . The dynamics of the counting process can be modeled using both exogenous and endogenous features. Here, *exogenous* refers to factors external to the temporal hypergraph, while *endogenous* refers to factors arising from within it. To capture these dynamics, we incorporate the *event history* at time t in the sub- σ -algebra $\mathcal{H}_t = \sigma(\{(t_m, I_m, J_m) \mid t_m \leq t\})$. If exogenous information is available, it should be included in the *filtration* $\mathbb{H} = \{\mathcal{H}_t\}_{t \geq 0}$.

Under the assumptions that make $N(\cdot, I, J)$ a right-continuous sub-martingale, adapted to the filtration \mathbb{H} , we can apply the *Doob-Meyer theorem* [Perry and Wolfe, 2013] to decompose it into two parts: a *noisy component* $M(\cdot, I, J)$, and a *predictable component*, the *cumulative intensity process* $\Lambda(\cdot, I, J)$. If it exists, the *intensity function* is defined as $\lambda(t, I, J) = \frac{\partial \Lambda(t, I, J)}{\partial t}$. This function describes the *instantaneous rate* at which the hyperevent (t, I, J) occurs. We decompose this rate as follows:

$$\lambda(t, I, J; \mathcal{H}_{t-}) = W(t, I, J) \cdot \lambda_0(t) \cdot \exp\{f(\mathbf{x}(t, I, J), t)\}, \quad (2)$$

where $\mathcal{H}_{t-} = \sigma(\{(t_m, I_m, J_m) \mid t_m < t\})$. This formulation is consistent with existing relational event and hyperevent models [Bianchi et al., 2024]. The term $W(t, I, J)$ is the *risk indicator*, which determines whether the pair (I, J) is at risk of a hyperevent at time t . The term $\lambda_0(t)$ is the *baseline hazard*, representing the baseline rate of event occurrence,

³The code required to implement the empirical analysis is provided in the Supplementary Material.

which may vary over time. The main focus of this paper is the *edge-specific contribution function*, $f(\mathbf{x}(t, I, J), t)$, which captures the effect of covariates on the event rate. In the next section, we discuss its specification and interpretation in detail.

2.2 Effects in Relational Hyperevent Modeling

The contribution function examines how edge-specific *covariates* influence the event occurrence rate. Although the true multivariate *covariate process* $X(t, I, J)$ is unobserved, we can observe p -dimensional samples through the vector of *measured covariates* $\mathbf{x}(t, I, J)$. The vector $\mathbf{x}(t, I, J)$ may include *exogenous covariates*, such as attributes of the senders and/or receivers. For example, in a bibliometric hyper-relational graph of authors and papers, one might use aggregate statistics related to authors' demographics, academic titles, or institutional affiliations as exogenous covariates. In this study, however, we primarily focus on *endogenous covariates*. In particular, we highlight a key aspect of event history modeling known as *subset repetition* [Lerner et al., 2025].

Subset repetition allows for flexible evaluation of social structures based on past events, counting interactions between subgroups of participants over time. To define subset repetition, we begin by quantifying the frequency of interactions between two sets of participants using the *activity operator*:

$$\text{activity}(t, I, J) = \sum_{t_m < t} \mathbb{1}_{\{I \subseteq I_m \cap J \subseteq J_m\}}, \quad (3)$$

where $\text{activity}(t, I, J)$ counts the number of past events in which all nodes in I (possibly with additional senders) jointly interacted with all nodes in J (possibly with additional receivers). Subset repetition of order (ρ, ℓ) is then defined as the average number of sender-to-receiver interactions for all subsets of senders of size ρ and receivers of size ℓ :

$$\text{subrep}^{\rho, \ell}(t, I, J) = \sum_{(I', J') \in \binom{I}{\rho} \times \binom{J}{\ell}} \frac{\text{activity}(t, I', J')}{\binom{|I|}{\rho} \times \binom{|J|}{\ell}}, \quad (4)$$

where $\binom{H}{\rho}$ denotes the set of all subsets of H of size ρ , and $\binom{|H|}{\rho}$ is the number of such subsets. In this work, we use the repeated interaction of sender and receiver subgroups — captured through subset repetition — as one of the key components for explaining hyperevent occurrences.

RHEM formulations in the current state of the art typically rely on the *linearity assumption*, which assumes that the contribution function is time-invariant and linear in the covariate values. A *linear model* is expressed as $f^{\text{LE}}(\mathbf{x}(t, I, J), t) = \boldsymbol{\theta}^\top \mathbf{x}(t, I, J)$, where $\boldsymbol{\theta}$ is a vector of unknown coefficients expressing the time-invariant linear effect (LE) of covariates $\mathbf{x}(t, I, J)$. We aim to relax this assumption by allowing each covariate to contribute in a non-linear way, with effects that may also vary over time. In the relational event modeling literature, more flexible specifications — such as time-varying or non-linear effects — have already been explored [Bauer et al., 2022, Boschi et al., 2025, Filippi-Mazzola and Wit, 2024b]. Our goal is to extend these approaches to the relational hyperevent modeling framework, allowing covariate effects that are *jointly* non-linear and time-varying. We first introduce the mathematical formulations for time-varying effects and non-linear effects, followed by the joint time-varying non-linear effect (TVNLE).

For the remainder of this modeling section, we focus on the contribution of a single covariate $x(t, I, J) \in \mathbf{x}(t, I, J)$ to the log-rate, denoted by $f^\square(x(t, I, J), t)$. For simplicity, we sometimes omit the dependence on $x(t, I, J)$ and t , writing f^\square instead. The symbol \square indicates whether the contribution is time-varying ($\square = \text{TVE}$), non-linear ($\square = \text{NLE}$), or jointly time-varying and non-linear ($\square = \text{TVNLE}$). Under the *additivity assumption*, the overall contribution function is expressed as $f(\mathbf{x}(t, I, J), t) = \sum_{k=1}^p f^{k, \square}(x^k(t, I, J), t)$, where $x^k(t, I, J)$ is the k -th covariate in the vector $\mathbf{x}(t, I, J)$, and $f^{k, \square}$ is its corresponding effect function. Each $f^{k, \square}$ is assumed to be a *smooth function*.

Time-varying effect. The contribution of a covariate with a time-varying effect can be expressed as:

$$f^{\text{TVE}}(x(t, I, J), t) = \alpha(t) \cdot x(t, I, J), \quad \alpha(t) = \sum_{l=1}^L \alpha_l a_l(t), \quad (5)$$

where $\alpha(t)$ is a *smooth function of time* evaluated at t and representing the TVE of $x(t, I, J)$. In its simplest form, α is represented as a linear combination of L non-linear basis functions of time a_l , each weighted by a coefficient α_l . Note that f^{TVE} is linear with respect to the covariate value. Thus, f^{TVE} is the product of a smooth function of time evaluated at t and the covariate value at time t . We generally refer to smooth function of time t as f_t .

Non-linear effect. Non-linear effects allow the impact of a covariate to vary across different levels. For example, a covariate's effect may increase up to a certain threshold, then plateau or even decrease beyond that point. The contribution of a covariate with a non-linear effect can be expressed as:

$$f^{\text{NLE}}(x(t, I, J)) = \sum_{q=1}^Q \beta_q b_q(x(t, I, J)). \quad (6)$$

Here, f^{NLE} is a *smooth function of the covariate* evaluated at time t . In its simplest form, f^{NLE} is represented as a linear combination of Q non-linear basis functions b_q , each weighted by a coefficient β_q . We generally refer to smooth function of covariate x as f_x .

We aim to introduce a novel type of effect that, to the best of our knowledge, has not yet been explored in either the relational event or relational hyperevent modeling frameworks. Specifically, we propose using tensor products as smooth functions of several variables [Wood, 2017] — particularly time and covariate — to model the joint time-varying non-linear effect of the covariate on event occurrence. The contribution of a covariate with a TVNLE can be expressed as:

$$f^{\text{TVNLE}}(x(t, I, J), t) = \sum_{q=1}^Q \left(\sum_{l=1}^L \alpha_{ql} a_l(t) \right) b_q(x(t, I, J)). \quad (7)$$

by allowing the coefficients β_q in Equation (6) to vary smoothly in time, expressing them as smooth functions of time as in Equation (5). We generally refer to smooth function of time t and covariate x as f_{tx} .

There are several options for the choice of spline basis functions in Equations (5), (6), and (7). In this paper, we focus on *thin plate regression splines* (TPRS), which are the default choice in the `mgcv` package in R [Wood, 2017]. While a comprehensive comparison of alternative spline types is beyond the scope of this work, we refer interested readers to Wood [2017] for a detailed discussion. Our primary aim is indeed to underline the importance of incorporating flexible effect specifications in the modeling of relational hyperevents.

Mathematical considerations about the model. TPRS are constructed by transforming and truncating the basis functions obtained from a *thin plate spline* (TPS) smoothing problem [Wood, 2003]. Within the TPS bases, two functions span the subspace of completely smooth terms [Wood, 2017]: one is constant over the input variable, and the other is linear, perfectly correlated with the input variable itself. When modeling a time-varying effect $\alpha(t)$, as in Equation (5), these basis functions include a constant term of the form $\alpha_l a_l(t) = \alpha_l a_l$, where a_l is constant in time. This term behaves like a time-invariant coefficient, representing the effect the covariate would have under a standard linear assumption. In the case of a non-linear effect, as in Equation (6), the contribution f^{NLE} is expressed as a linear combination of basis functions of the covariate, $\beta_q b_q(x)$. When the basis function $b_q(x)$ is linear, the term $\beta_q b_q(x) = \beta_q b_q \cdot x$ corresponds to a linear effect, up to a linear transformation of the covariate itself. This structure can also show that both TVE and NLE can be interpreted as restricted versions of TVNLE, defined in Equation (7). If only the constant basis terms in time are active, the effect becomes non-linear in the covariate but time-invariant. Conversely, if only the linear basis terms in the covariate are retained, the effect becomes time-varying but linear in the covariate.

2.3 Inference Procedures

To implement the estimation procedure based on the data in Equation (1), we use a sampled version of the *partial likelihood* [Lerner and Lomi, 2020]. Specifically, at each event time, we consider only two instances: the observed hyperevent that actually occurred, and a *non-hyperevent* — an event that did not occur but could have — randomly sampled from those at risk.

Conditioning each observation on the event history and the corresponding event time, the *case-control partial likelihood* can be expressed as:

$$\begin{aligned} \mathcal{L}(\boldsymbol{\theta}) &= \prod_{m=1}^n \frac{\exp \{f(\mathbf{x}(t_m, I_m, J_m); \boldsymbol{\theta})\}}{\exp \{f(\mathbf{x}(t_m, I_m, J_m); \boldsymbol{\theta})\} + \exp \{f(\mathbf{x}(t_m, I_m^*, J_m^*); \boldsymbol{\theta})\}} \\ &= \prod_{m=1}^n \text{logistic}[f(\mathbf{x}(t_m, I_m, J_m); \boldsymbol{\theta}) - f(\mathbf{x}(t_m, I_m^*, J_m^*); \boldsymbol{\theta})], \end{aligned} \quad (8)$$

where (I_m^*, J_m^*) denotes the sender and receiver sets of a non-hyperevent sampled at time t_m . In our empirical application, the non-event is constrained to have the same sender and receiver cardinalities as the observed event, i.e., $(I_m^*, J_m^*) \in \binom{V_{t_m}^I}{|I_m|} \times \binom{V_{t_m}^J}{|J_m|}$. Here, $\boldsymbol{\theta}$ denotes the vector containing all coefficients associated with the basis functions

used to represent the smooth covariate effects, or, in the special case of a linear effect, the single coefficient associated with the covariate. Following Boschi et al. [2025], Equation (8) corresponds to the likelihood of a degenerate logistic regression, where the response is fixed (equal to 1), the intercept is omitted, and the predictors are given by the difference in the contribution function evaluated between the observed event and the sampled non-event. As a result, we can fit our model as a *Generalized Additive Model* (GAM), rather than relying on traditional survival modeling techniques.

To reduce potential overfitting, especially when using smooth functions, we employ a *penalized likelihood* as the objective function:

$$\mathcal{L}^\tau(\boldsymbol{\theta}) = \mathcal{L}(\boldsymbol{\theta}) - \sum_{k=1}^p \tau^k P^k(f^{k,\square}), \quad (9)$$

where each of the p smooth terms is penalized through an associated *penalty term* P^k , with the exception of covariates modeled with a linear effect, for which the penalty is set to zero. The penalty term is weighted by the relative *smoothing parameter*, controlling the trade-off between model fit and smoothness. Smoothing parameters are stored in vector $\boldsymbol{\tau}$.

For a univariate smooth effect f^{NLE} , also denoted by f_x , a common penalty is $P(f_x) = \int \left(\frac{\partial^2 f_x}{\partial x^2} \right)^2 dx$, which quantifies the *wigginess* of the function. As $\tau \rightarrow \infty$, the function f_x is increasingly constrained toward linearity, ultimately reducing to a straight line. More complex penalty expressions are used in the case of TPRS. However, expressing f_x as a linear combination of basis functions, as in Equation (6), allows each penalty $P_x(f_x)$ to be written as a quadratic form in the corresponding coefficient vector.

When dealing with multivariate smooth functions — and in particular, with functions of both time and covariate, as in our main case of interest — we denote the TVNLE effect by f_{tx} . The associated penalty can be expressed as:

$$P(f_{tx}) = \tau_t \int_x P(f_{t|x}) dx + \tau_x \int_t P(f_{x|t}) dt$$

where τ_t and τ_x control the the tradeoff between wigginess in different directions and $f_{t|x}$ is f_{tx} considered as function t , holding x constant. If we refer to the previously mentioned $P(f_x)$ used as an example, the penalty term in the multivariate case would be $P(f_{tx}) = \int_{t,x} \tau_t \left(\frac{\partial^2 f_{tx}}{\partial t^2} \right)^2 + \tau_x \left(\frac{\partial^2 f_{tx}}{\partial x^2} \right)^2 dt dx$ [Wood, 2017]. Estimation of $\boldsymbol{\tau}$ is usually performed via *cross-validation*.

3 Simulation study

To validate our approach and demonstrate its potential, we apply it to synthetic hyperevent data. We generate undirected hyperevents of the form $(t_m, I_m, J_m = \emptyset)$, representing meetings. Each meeting involves a varying number of participants in I_m , with event sizes ranging from 1 up to a predefined maximum w , which defines the largest possible event ($|I_m| \leq w \forall m$). Events are generated from a known underlying model, as described in Equation (2). We consider four explanatory variables. Two are endogenous covariates, represented by first- and second-order subset repetition covariates (as defined in Equation (4) with $\rho = 1, 2$, respectively). One exogenous covariate corresponds to the average of a quantitative feature evaluated across all meeting participants (i.e., nodes in the hyperedge). This individual-level feature is drawn from a Gaussian distribution, with its mean and standard deviation defined as part of the simulation setup. Lastly, event size is included as an explanatory variable, modeled as a size penalty: it contributes negatively to the log-occurrence rate of the hyperevent.

For each simulated hyperevent, we allow the corresponding non-observed meeting to take any possible size from 1 to w . This setup offers greater flexibility compared to the strategy adopted in our empirical application, where non-hyperevents are sampled to match the size of the observed hyperevent. In particular, allowing variation in non-event sizes enables us to estimate the effect of event size. However, this flexibility is feasible primarily because we are working with a relatively small hypergraph. As the number of actors increases, the number of possible hyperedges grows exponentially, making this approach computationally infeasible at larger scales.

Depending to the simulation setup, covariates effects are selected as LE, TVE, NLE, and TVNLE. This study was designed with four objectives in mind. First, we aim to demonstrate that when the true underlying effect is linear, both NLE and TVNLE specifications are flexible enough to recover linearity as a special case, as discussed in Section 2.2. Second, we highlight that when the true effect varies over time, fitting a linear model fails to capture the temporal dynamics accurately. Third, we show the potential of the proposed joint TVNLE estimation procedure in capturing complex covariate effects. Finally, we emphasize that using only time-varying or only non-linear models may be insufficient when the data-generating process involves both temporal and non-linear components.

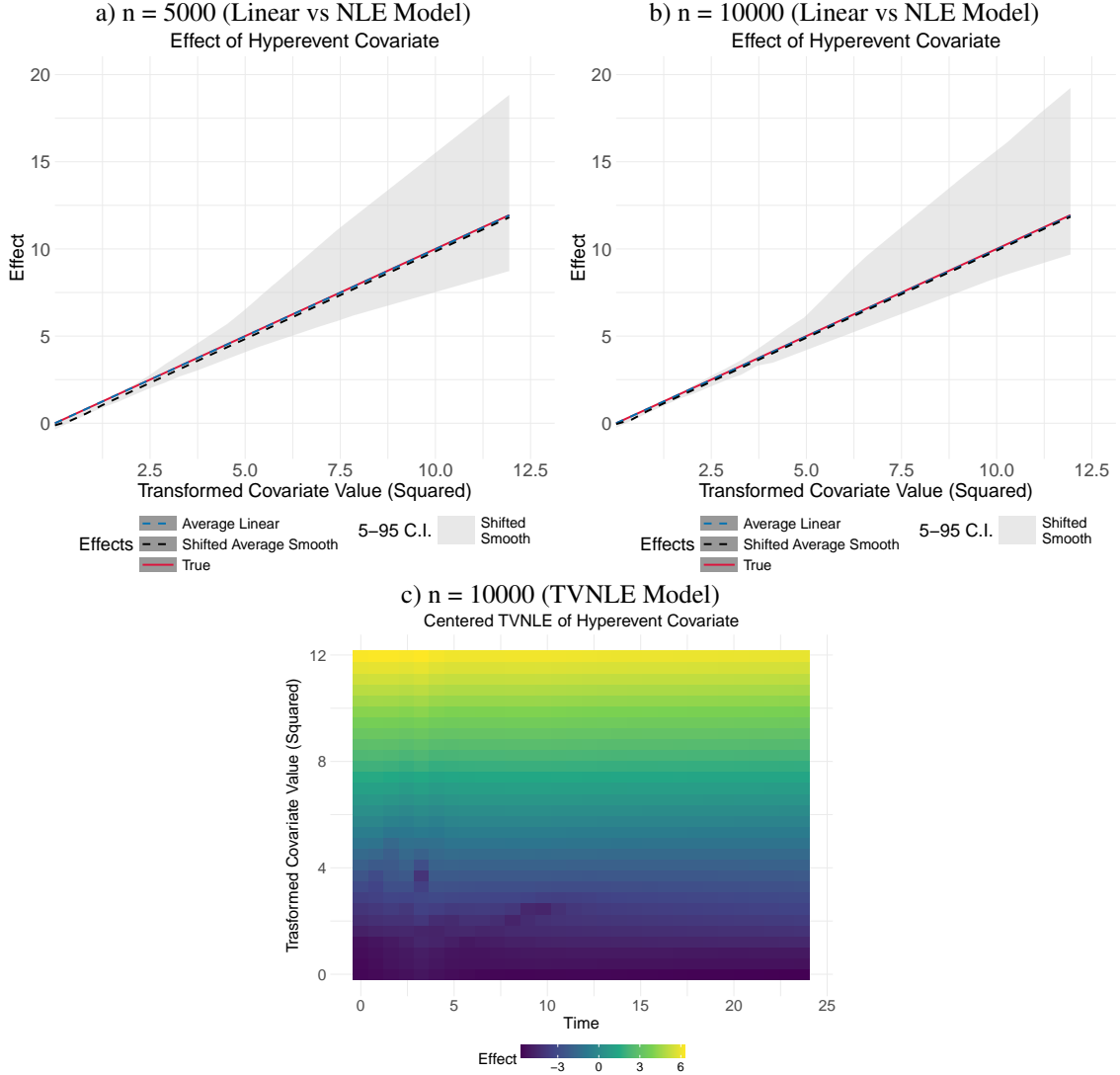


Figure 1: Linear models are recovered by penalized non-linear models. Panels a), b), and c) display results based on synthetic data generated according to the model in Equation 10, differing only in the number n of simulated events. Panels a) and b) show estimates from linear and non-linear models, while panel c) presents results from a model incorporating a joint time-varying and non-linear effect. *Top.* Across experiment replications, estimates are aggregated using inverse variance weighting. For the linear model, this yields a consensus slope referred to as the “consensus linear effect” (blue dashed line). For non-linear models, predicted effects are interpolated across the covariate domain, and aggregated pointwise using inverse variance weights, resulting in the “consensus non-linear effect” (black dashed line). Since non-linear estimates are identifiable only up to an additive constant, the consensus curve is manually shifted for alignment. Confidence intervals, derived from the 5th and 95th percentiles of the empirical interpolated estimates at each covariate value, are also shifted accordingly. Both linear and non-linear estimated effects are compared to the ground truth (red solid line). *Bottom.* For the TVNLE model, estimates are aggregated using inverse variance weighting. The resulting smooth surface is then centered such that, at each time point, the average effect across the covariate domain is equal to 0.

Each simulation scenario presented in this study is replicated 100 times. Since the synthetic datasets differ across replications, the observed ranges of both time and covariate values may vary accordingly. As a consequence, some predicted values may correspond to out-of-sample observations for models that were fitted on more limited ranges of the covariate or time.

Linear models are recovered by penalized non-linear models. We generate synthetic hyperevent data according to the following underlying model:

$$\lambda(t, I) = -\log \left(\sqrt{\text{subrep}^1(t, I)} \right) + \log \left(\sqrt{\text{subrep}^2(t, I)} \right) + \bar{x}(I)^2 - 0.5 \cdot |I|. \quad (10)$$

Simulated hyperevents represent undirected meetings involving multiple interacting actors, without distinguishing between senders and receivers. Consequently, the intensity function depends solely on the set I of participants. The terms $\text{subrep}^1(t, I)$ and $\text{subrep}^2(t, I)$ are endogenous covariates capturing first- and second-order subset repetition, respectively, as defined in Equation (4). The variable $\bar{x}(I)$ is an exogenous covariate computed as the average of a Gaussian-distributed individual feature across all members of I . Finally, $|I|$ denotes the size of the meeting, included in the model with a negative contribution to penalize larger events. If $\bar{x}(I)^2$ is used as the covariate — instead of $\bar{x}(I)$ — its effect remains linear within the model specification, as the transformation is applied to the covariate before modeling.

Figure 1 aggregates both linear and non-linear estimates from multiple replications using *inverse-variance weighting* [Hartung et al., 2011].

Specifically, for the linear model, we aggregate the estimated slopes. For non-linear effects, we first interpolate the predicted effects over the covariate values, then perform point-wise aggregation, weighting each contribution inversely by its corresponding variance. Since estimated non-linear functions are interpretable only in terms of their trend, rather than their absolute sign or value, we manually shifted the consensus line (and relative confidence intervals) to facilitate direct comparison with the true and linear model estimates. As shown in Figure 1 a) and b), the flexible model successfully captures the true linear trend. Also, comparing results for different numbers of meetings n , we can see that as n increases, there is a reduction in the variability of the non-linear estimates across different replications.

Similarly, we interpolate joint time-varying non-linear effects using inverse-variance weighting. Furthermore, since TVNLE can only be identifiable up to the addition of an arbitrary function $f_0(t)$, depending on time but not on the covariate, we center the value in such a way that they have zero-mean for each value of time. The fitted TVNLE models successfully recover a linear, time-invariant trend, as shown in Figure 1 c). Linearity can be seen by fixing a point on the x -axis (time t) and observing that the effect values vary monotonically with covariate values on the y -axis, increasing from bottom to top. Time-invariance is confirmed by fixing a point on the y -axis (covariate value) and noting that the effect remains essentially constant, from left to right, over time.

Linear models fail to capture time-varying effects. We simulate hyperevent data from the true underlying model with time-varying effects,

$$\lambda(t, I) = \underbrace{-10 \cdot t \cdot \log \left(\sqrt{\text{subrep}^1(t, I)} \right)}_{\beta_1(t)} + \underbrace{10 \cdot t \cdot \log \left(\sqrt{\text{subrep}^2(t, I)} \right)}_{\beta_2(t)} + \underbrace{10 \cdot t \cdot \bar{x}(I)^2}_{\beta_3(t)} - \underbrace{0.1 \cdot |I|}_{\beta_4}. \quad (11)$$

Here, $\beta_j(t)$ for $j = 1, 2, 3$ are time-varying functions. By contrast, the true effect of event size $\beta_4 < 0$ is time-invariant and linear. Figure 2 shows that the linear model fails to capture the time-varying effect of this variable. By contrast, the TVE model successfully identifies it. The TVNLE model also correctly identifies the time-varying — but, for each time point, linear — effect. As it can be seen, for time equal to zero, the effect does not increase with the covariate (constant color on the vertical line at $t = 0.0$), while the vertical color gradient becomes steeper as time increases.

The potential of the joint time-varying non-linear estimation. In the previous analysis, we assumed knowledge of the true non-linear transformation of the covariate, applying it explicitly in the model. This is clearly unrealistic in practice. In this third section, we therefore remove the known square transformation of $\bar{x}(I)$ — which we know to be the true form — and instead allow the transformation to be learned from the data itself, permitting it to vary over time.

Figure 3 shows the true centered effect (*Top Left*), i.e. $f^{\text{TVNLE}}(\bar{x}(I), t) = +10 \cdot t \cdot \bar{x}(I)^2$ and the estimated effect $\hat{f}^{\text{TVNLE}}(\bar{x}(I), t)$ (*Top Right*). The color shading represents the effect, plotted with time t on the x-axis and the values of the hyperevent covariate $\bar{x}(I)$ on the y-axis. We observe that the estimates successfully capture both the variation over time and the variation across covariate values. The image was generated by predicting the log-hazard contributions for 30 pairs of time and covariate values, uniformly sampled from the range of the synthetic data.

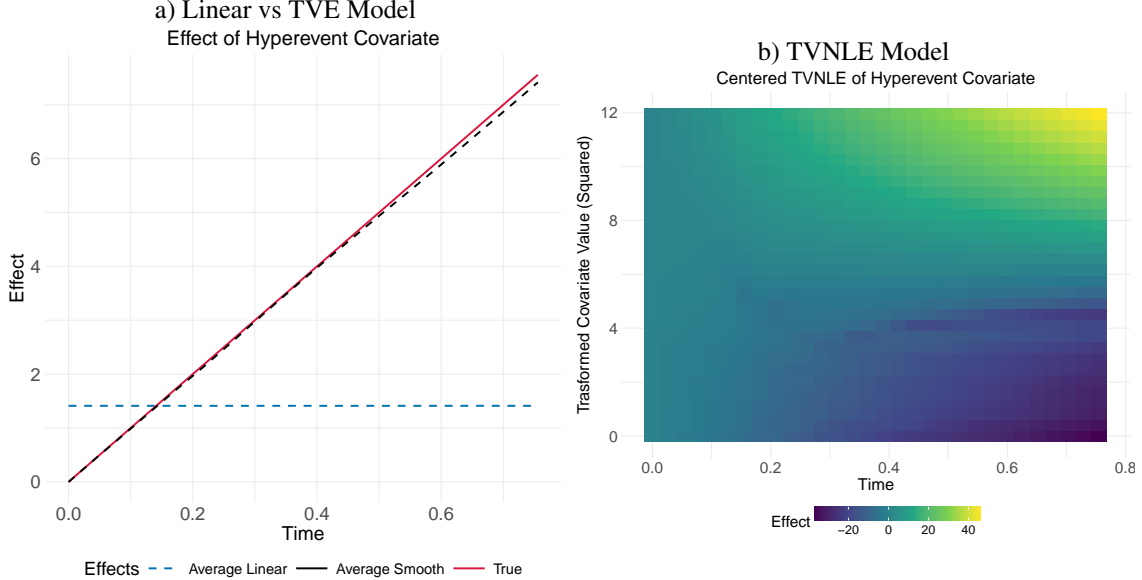


Figure 2: Linear Models Fail to Capture Non-Linear Effects. Panels a) and b) display results based on synthetic data generated according to the model in Equation 11. Panels a) shows estimates from linear and time-varying models, while panel b) presents results from a model incorporating a joint time-varying and non-linear effect. a) Estimates from multiple replications are combined using inverse variance weighting. For the linear model, we aggregate the estimated slopes to create a consensus line, called the “consensus linear effect” (blue dashed line). Unlike Figure 1, the x-axis here shows time. As a result, the consensus linear effect appears as a horizontal line, since it does not change over time. In contrast, the true effect (red solid line) changes over time. Linear models cannot capture this time-dependent pattern. For time-varying effects, we first interpolate predicted effects across time points. Then, we aggregate them pointwise, weighting each by the inverse of its variance. This produces a “consensus time-varying effect” (black dashed line) that captures the average time trend well. Notably, unlike in Figure 1, the sign of the effect here can be interpreted. Therefore, the consensus non-linear effect is not shifted. b) For the TVNLE model, estimates are aggregated using inverse variance weighting. The resulting smooth surface is then centered such that, at each time point, the average effect across the covariate domain is equal to 0.

Time-varying and non-linear models fail to capture simultaneous time-varying non-linear effects. Figure 3 *Bottom Left* and *Bottom Right* displays interpolated values of the estimated contributions to the log-rate function, obtained by fitting a model with time-varying effects and non-linear effects only. It is important to note that when considering TVE, the log-hazard contribution corresponds to the time-varying effect multiplied by the value of the covariate at the corresponding time. We observe that the TVE contribution incorrectly identifies a decrease in the value of the contribution for low covariate values towards the end of the time window. In contrast, the NLE model fails to capture the temporal variation in the data.

4 Empirical Application to Coauthorship Citation Networks

We applied our RHEM extension to the DBLP-Citation-network V14 dataset, restricted to journal articles, derived from the Aminer Citation Network [Tang et al., 2008]. In this context, a relational hyperevent is defined as the formal *publication of a scientific work*, marking the moment when a group of authors presents their research alongside a set of citations listed in the reference section. Our analysis is specifically focused on journal publications, constructing an event list that includes only these types of works. Furthermore, among the cited works, we also restrict our selection to journal publications to maintain consistency within the dataset. The resulting event sequence comprises $n = 1,416,353$ publication events spanning from 1939 to 2023.

$$\{j_m = (t_m, I_m, J_m), m = 1, \dots, 1416,353\}$$

Here, j_m represents the journal article published at time t_m by a group of authors in $I_m \subseteq V_{t_m}^I$ citing journal articles in $J_m \subseteq V_{t_m}^J$. This dataset was previously analyzed using a standard linear RHEM approach [Lerner et al., 2025]. We selected it as an empirical test case to demonstrate the advantages of our proposed model over the current state-of-the-art

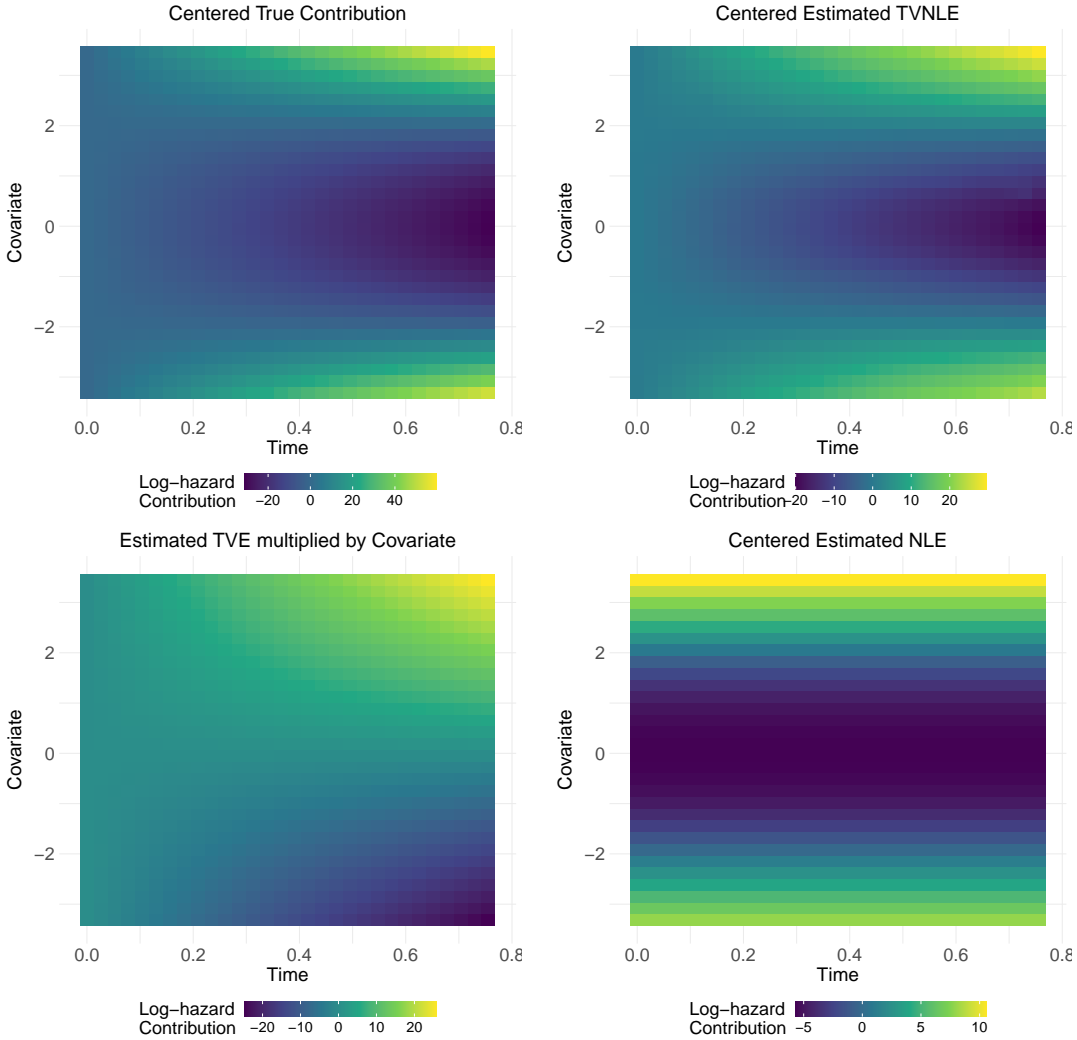


Figure 3: The potential of joint time-varying non-linear estimation and the failure of time-varying and non-linear models. The four plots display results from simulated data based on the model in Equation 11. The two upper plots in Figure 3 show centered true effect and the estimated effect, respectively. The color shading represents the effect $f^{\text{TVNLE}}(\bar{x}(I), t)$, with time t on the x-axis and the values of the hypercovariate $\bar{x}(I)$ on the y-axis. The two lower plots in Figure 3 show interpolated values of the estimated contributions to the log-rate function, obtained by fitting a model with only time-varying effects and non-linear effects, respectively. The contribution to the log-rate with TVE consists of the TVE itself multiplied by the value of the covariate at the corresponding time.

methodology as represented by the cited study. Code to preprocess and filter the data is publicly available.⁴ The counting process $N(t, I, J)$ tracks the cumulative number of papers authored by group I that cite works in set J up to time t . This approach examines how endogenous relational mechanisms — particularly prior scientific collaborations or citation patterns among authors — influence the publication rate of journal articles.

The inclusion of time-varying effects is particularly pertinent in this analysis, given that publication events are not uniformly distributed: over 87% of the publications occurred after 2000. By including in the model formulation an explicit reference to the time of the event, interacting with the covariate evaluated at the time of interest, our technique allows to account for this temporal imbalance. Moreover, this empirical application carries significant social implications. Scientific networks provide insights into the factors motivating different authors to collaborate, revealing the complex dynamics that drive co-authorship and knowledge exchange. This presents a valuable opportunity to deepen our understanding of the evolving dynamics within complex social networks, particularly within the scientific domain. These networks consist of interconnected authors and papers, but they can also include inventors, awardees, investors, publications, grants, and patents, along with their intricate relationships. Such networks are continually expanding, embodying social phenomena like the exchange of funding, knowledge, and reputation. There is no inherent justification for assuming that this influence is linear or homogeneous over time, as collaboration patterns evolve in response to shifts in research interests, available resources, and community structures, as demonstrated in various approaches to analyzing co-authorship networks [Hoekman et al., 2010, Kwiek, 2021].

4.1 Drivers of Scientific Collaboration and Impact

Using the case-control partial likelihood inference framework with GAMs, as explained in Section 2.3, we sampled one possible but unobserved event from the risk set for each publication event. For each group of authors I and the corresponding group of cited papers J at time t , we selected a pair $(I^*, J^*) \in \binom{V_t^I}{|I|} \times \binom{V_t^J}{|J|}$, ensuring both groups have the same size in the hyper-event and the non-hyperevent. Hyperedge covariates were generated using the open-source software `eventnet` Lerner and Lomi [2020, 2023],⁵ which allows sampling a specified number of non-event hyperedges related to each observed publication event, and calculating covariates for both observed events and sampled non-events. In our analysis, we sample one non-event ($m = 1$).

In this empirical application, relational hyperevents represent *citations*. Therefore, we replace the generic term “action” in Equation (3) with “citation”. We focus on a subset of the hyperedge covariates studied in Lerner et al. [2025] and, following that work, incorporate a weight factor ω to model the temporal decay of past events. Most of the statistics used can be defined by adapting and combining the function “citation”. Specifically, we introduce the following adaptations, based on the superscript referring to either authors or papers (aut or pap):

1. *Author-Paper citations*:

$$\text{cite}^{\text{aut-pap}}(t, I, J) = \sum_{t_m < t} \omega(t - t_m) \cdot \mathbb{1}_{\{I \subseteq I_m \cap J \subseteq J_m\}}$$

2. *Paper-paper citations*:

$$\text{cite}^{\text{pap-pap}}(t, j, j') = \sum_{t_m < t} \omega(t - t_m) \cdot \mathbb{1}_{\{j = j_m \wedge j' \in J_m\}}$$

3. *Author-Author citations*:

$$\text{cite}^{\text{aut-aut}}(t, i, i') = \sum_{t_m < t} \omega(t - t_m) \cdot \mathbb{1}_{\{i \in I_m \wedge \exists t_{m'} : j_{m'} \in J_m \wedge i' \in I_{m'}\}}$$

4. *Author citation popularity*:

$$\text{cite_pop}^{\text{aut}}(t, i) = \sum_{t_m < t} \omega(t - t_m) \cdot \mathbb{1}_{\{\exists t_{m'} : j_{m'} \in J_m \wedge i \in I_{m'}\}}$$

5. *Authorship*:

$$\text{author}(t, i, j) = \sum_{t_m < t} \omega(t - t_m) \cdot \mathbb{1}_{\{j = j_m \wedge i \in I_m\}}$$

⁴https://github.com/juergenlerner/eventnet/tree/master/data/scientific_networks/aminer_2023

⁵<https://github.com/juergenlerner/eventnet>

6. *Out-degree*:

$$\text{out_degree}(j) = \sum_{t_m} \omega(t - t_m) \cdot \mathbb{1}_{\{j=j_m\}} \cdot |J_m|,$$

where $\omega(t - t_m) = \exp\{-(t - t_m) \frac{\log 2}{T_{\frac{1}{2}}}\}$ and $T_{\frac{1}{2}} > 0$ is the half-life period [Lerner et al., 2013].

As we show that “action” defined in Equation (3) serves as a basic block for subset-repetition “subrep” defined in Equation (4), all the previously listed adaptations play a similar role. Specifically, we focus our attention on the following hyperedge covariates involving authors’ network, papers’ network and their interconnection (see Lerner et al. [2025] for a more detailed description, graphical illustration, and numerical examples).

1. *Prior papers*:

$$\text{prior_papers}(t, I, J) = \text{subrep}^{(1,0)}(t, I, J)$$

2. *Prior joint papers*:

$$\text{prior_joint_papers}(t, I, J) = \text{subrep}^{(2,0)}(t, I, J)$$

3. *Paper citation popularity*:

$$\text{paper_citation_popularity}(t, I, J) = \text{subrep}^{(0,1)}(t, I, J)$$

4. *Paper pair co-citation*:

$$\text{paper_pair_cocitation}(t, IJ) = \text{subrep}^{(0,2)}(t, I, J)$$

5. *Author citation repetition*:

$$\text{author_citation_repetition}(t, I, J) = \text{subrep}^{(1,1)}(t, I, J)$$

6. *Cite paper and its references*:

$$\text{cite_paper_and_its_references}(t, I, J) = \sum_{\{j, j'\} \in \binom{J}{2}} \frac{\text{cite}^{\text{pap-pap}}(t, j, j') + \text{cite}^{\text{pap-pap}}(t, j', j)}{\binom{|J|}{2}}$$

7. *Difference in prior papers*:

$$\text{difference_in_prior_papers}(t, I, J) = \sum_{\{i, i'\} \in \binom{I}{2}} \frac{|\text{cite}^{\text{aut-pap}}(t, \{i\}, \emptyset) - \text{cite}^{\text{aut-pap}}(t, \{i'\}, \emptyset)|}{\binom{|I|}{2}}$$

8. *Author citation popularity*:

$$\text{author_citation_popularity}(t, I, J) = \sum_{i \in I} \frac{\text{cite_pop}^{\text{aut}}(t, i)}{|I|}$$

9. *Difference in author citation popularity*:

$$\text{difference_in_author_citation_popularity}(t, I, J) = \sum_{\{i, i'\} \in \binom{I}{2}} \frac{|\text{cite_pop}^{\text{aut}}(t, i) - \text{cite_pop}^{\text{aut}}(t, i')|}{\binom{|I|}{2}}$$

10. *Collaborate with citing author*:

$$\text{collaborate_with_citing_author}(t, I, J) = \sum_{\{i, i'\} \in \binom{I}{2}} \frac{\text{cite}^{\text{aut-aut}}(t, i, i') + \text{cite}^{\text{aut-aut}}(t, i', i)}{\binom{|I|}{2}}$$

11. *Author self citation*:

$$\text{author_self_citation}(t, I, J) = \sum_{i \in I, j \in J} \frac{\text{author}(i, j)}{|I| \cdot |J|}$$

12. *Paper outdegree popularity*:

$$\text{paper_outdegree_popularity}(t, I, J) = \sum_{j \in J} \frac{\text{out_degree}(j)}{|J|}$$

To improve model fitting stability, we modified the network statistics by using a different approach from the square-root transformation proposed in Lerner et al. [2025]. Similar to their goal, our aim is to reduce the effect of outliers on the model. To achieve this, each covariate—whether for observed events or non-events—is transformed using the following formula:

$$\dot{x}^k = 1 - \exp\left(-\frac{x^k}{c^k}\right) \quad (12)$$

Here, x^k is a value of the k -th covariate, observed for either events or non-events. The parameter c^k is selected through an optimization procedure. This procedure finds the value of c^k that brings the transformed covariate as close as possible to a uniform distribution, based on minimizing the Kolmogorov–Smirnov statistic. Additionally, we applied a transformation to the timing of the events. Since time is evaluated in the same way for both events and non-events, we used the *empirical cumulative distribution function* (ECDF) of the event times to transform them into a uniform distribution:

$$\dot{t} = \text{ecdf}_t(t)$$

where ecdf_t is the ECDF of the event times. Although these transformations may seem to make interpretation harder, after fitting we map values back to the original scale and interpret the results in terms of the original covariates.

4.2 Model fitting procedure

Following the modeling framework outlined in Section 2, we first assume a time-varying non-linear effect for each of the 12 covariates discussed in Section 4.1, contained in vector $\dot{x}(t, I, J)$, and transformed according to Equation (12). The contributions of these covariates to the log-hazard follows:

$$f(\dot{x}(t, I, J), \dot{t}) = \sum_{k=1}^{p=12} \sum_{q=1}^Q \left(\sum_{l=1}^L \alpha_{ql}^k a_l^k(\dot{t}) \right) b_q^k(\dot{x}^k(t, I, J))$$

In this expression, $f(\dot{x}(t, I, J), \dot{t})$ represents the contribution function expressing an additive joint time-varying non-linear effect of transformed covariates $\dot{x}(t, I, J)$ on the log-hazard function. Each effect, in its trend, and not its sign, can be interpreted as the effect of the original covariate $x_k(t, I, J)$ on the log-hazard function.

Fitting the complete model, we observed extreme values for the effect of the covariate “Prior joint papers.” On closer inspection, only a very small number of non-events took a value different from zero (18 out of 1,416,353). This indicates that, for a randomly selected potential event, it is rare to find a pair of actors with previous co-authorship. In contrast, events often show nonzero values for this covariate. To avoid unstable non-linear estimates, we chose to include a linear effect for this covariate.

Excluded Covariate	AIC Difference	LogLik Difference	Deviance Difference
Difference in prior papers	-3886.01	1955.02	-3910.04
Author citation popularity	-2858.46	1435.35	-2870.69
Difference in author citation popularity	-408.09	215.52	-431.04
Paper outdegree popularity	-433.07	232.89	-465.77
Prior papers	-19288.83	9651.47	-19302.94
Prior joint papers (Linear)	-3210100.35	1605046.84	-3210093.69
Collaborate with citing author	-341.42	176.77	-353.54
Paper citation popularity	-34990.31	17508.85	-35017.71
Paper pair cocitation	-15622.95	7809.36	-15618.71
Author citation repetition	-6249.01	3134.45	-6268.9
Cite paper and its references	-19968.94	10001.37	-20002.73
Author self citation	-33584.8	16789.89	-33579.78

Table 1: Contribution of individual network attributes. For each row in the table, we report the difference in AIC, log-likelihood (LogLik), and deviance between the full model (including all 12 covariates) and a reduced model that excludes the covariate listed in that row. This value reflects the difference in log-likelihood between the full model and the reduced model.

To perform model selection, we explore only a subset of the nested models. Namely, for each of the 12 presented covariates, we fitted a model including all the other covariates. We then assessed the effect of each covariate by comparing the change in AIC and log-likelihood between the full and partial models. These differences can be evaluated in Table 1. All twelve effects lead to an improvement in the AIC. Therefore, our final model contains all the mentioned

covariates. To facilitate comparison with the baseline model assuming linear effects that are homogeneous over time, we fit standard RHEM Lerner et al. [2025] specified with the twelve effects; see Table 2.

4.3 Evolving Dynamics of Scientific Collaboration and Impact

We first consider the interpretation of the covariate ‘‘Prior joint papers,’’ which was included with a linear effect. The estimated coefficient is 421.93, with a standard error of 26.99. This shows a very strong, but not degenerate, effect of this variable. Furthermore, Table 1 highlights the importance of retaining this covariate in the model formulation.

In the Supplementary Materials (Section B), we provide all figures illustrating the TVNL effects for the covariates included in the final model formulation. In this section, we focus on the interpretation of some of these effects showing a specific behavior: either non-monotone, time-varying, non-monotone and time-varying, or (approximately) monotone and homogeneous over time. We emphasize monotone vs. non-monotone, rather than linear vs. non-linear, since any linear approximation of a truly non-monotone effect would actually lead to a seriously invalid interpretation: any linear effect assumes that a covariate is either increasing or decreasing the event rate throughout its entire range – while a non-monotone effect reveals that there are intervals in which the covariate increases the rate and other intervals in which it has a decreasing effect. One might argue that the practical implications of a non-linear, but strictly monotone effect are limited in many typical applications of relational event modeling, as analysts would still capture the correct direction of the effect.

It is important to note that the plots in the following figures should not be interpreted in terms of their sign. More precisely, the function $f^{\text{TVNLE}}(x(t, I, J), t)$ in Equation (7) is only identifiable up to the addition of a function $f_0(t)$ that may depend on time (but not on the covariate value $x(t, I, J)$). This is because any such function $f_0(t)$ would cancel out in each of the terms of the partial likelihood (8). Thus, using $f^{\text{TVNLE}}(x(t, I, J), t) + f_0(t)$ instead of $f^{\text{TVNLE}}(x(t, I, J), t)$ defines the same model. We have therefore centered the values displayed in the two-dimensional heatmap plots around zero for each time point.

Difference in prior papers. This covariate on a hyperedge (I, J) at time t is the average of the absolute pairwise differences in the number of previously published papers, taken over all pairs of authors in I . The baseline effect in Table 2 is positive, suggesting that teams of authors are typically composed of authors with large differences in the number of papers they have previously published, for example a PhD student together with her supervisor. The TVNLE plot in Figure 4 a) suggests a clearly non-monotone (hence non-linear) effect. If we fix a point on the horizontal axis (time) and go from bottom (covariate at its minimum value) to top (covariate at its maximal value), we find an increase in the event rate, up to about $x = 1.5$, but then a decrease in the event rate. This means that the linear pattern (more difference in the number of prior papers implies a higher event rate) holds only for the lower values but gets reversed for higher values. The non-monotone pattern is qualitatively similar over time – although the maximum is less pronounced at the end of the observation period and sharper at the beginning.

Cite paper and its references. This covariate on a hyperedge (I, J) at time t is the average number of prior citations among all pairs of papers in J . The baseline effect in Table 2 is strongly positive, suggesting a tendency to partially

	Estimate	Std. Error	z value	Pr(> z)
Difference in prior papers	0.85	0.03	30.84	0.00
Author citation popularity	-1.14	0.03	-39.33	0.00
Difference in author citation popularity	-0.70	0.03	-23.09	0.00
Paper outdegree popularity	0.32	0.01	24.49	0.00
Prior papers	-0.42	0.03	-15.76	0.00
Prior joint papers	440.00	21.12	20.83	0.00
Collaborate with citing author	1.66	0.02	77.51	0.00
Paper citation popularity	4.55	0.03	162.28	0.00
Paper pair cocitation	40.58	1.37	29.56	0.00
Author citation repetition	38.74	1.63	23.80	0.00
Cite paper and its references	31.07	1.39	22.36	0.00
Author self citation	47.56	1.92	24.82	0.00

Table 2: Summary of the baseline model. The baseline model includes a linear effect for each of the 12 covariates discussed in Section 4.1, contained in vector $\mathbf{x}(t, I, J)$, and transformed according to Equation (12). The contribution function, in this case, is $f^{\text{LE}}(\dot{\mathbf{x}}(t, I, J), t) = \boldsymbol{\theta}^\top \dot{\mathbf{x}}(t, I, J)$.

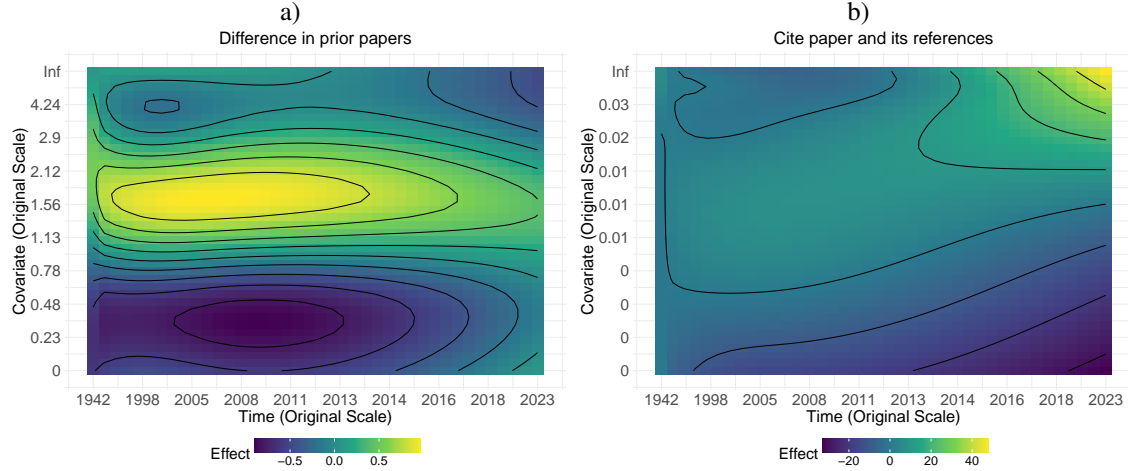


Figure 4: **Estimated TVNLE of Difference in Prior Papers and Cite Paper and Its References.** a) Estimated TVNLE (log-hazard contribution) of Difference in Prior Papers. The plot should be interpreted in terms of trend, not sign. The estimate suggests a non-monotonic and thus non-linear effect across the range of the covariate. Although the effect appears nearly constant over time (except in recent years), for each fixed point in time, the pattern shows an initial decrease, followed by an increase, and then another decrease along the covariate range. b) Estimated TVNLE (log-hazard contribution) of Cite Paper and Its References. The effect is estimated as almost linear and very strong toward the end of the observation period. Before 2014, the covariate shows a non-monotonic pattern—first increasing and then decreasing with the covariate value. This illustrates a clear example of a time-varying effect.

copy the reference list of cited papers. However, the TVNLE plot in Fig. 4 b) shows that this very strong effect mostly holds around the end of the observation period, while earlier the effect is much weaker. Prior to 2011 the covariate even has a slightly non-monotone effect that has an increasing effect on the event rate for low values of the covariate and a decreasing effect for high values. The tendency to cite a paper together with some of its references is thus an example of a time-varying effect. The finding that the tendency to cite a paper together with some of its references becomes very strong only at the end of the observation period could be of substantive interest as it gives support to the interpretation that increasing use of publication databases and paper-search technology might strengthen this effect [Lerner et al., 2025]. Since it becomes increasingly simple to follow paper citations forward and backward, and to retrieve the respective papers, the tendency to cite a paper and some of its references, or some of the papers previously citing it, may become stronger over time.

Author self-citation. This covariate on a hyperedge (I, J) at time t is the fraction of pairs $(i, j) \in I \times J$, such that i is among the authors of j . The baseline effect in Table 2 is strongly positive, suggesting that authors have a tendency to cite their own prior work. The TVNLE plot in Fig. 5(a) suggests a more complex pattern where an approximately monotone increase can be found only at the beginning and end of the observation period, while for time in the interval [2008, 2016] the effect is clearly non-monotone, first increasing for low values of the covariate and then decreasing for high values. This covariate is thus an example of an empirical effect that is jointly time-varying and non-monotone.

Paper citation popularity. We have also found effects that are approximately monotone and nearly constant over time. The covariate “paper citation popularity” on a hyperedge (I, J) at time t is the average number of prior citations received by the papers in J . The baseline effect in Table 2 is positive, revealing the well-known “preferential attachment” or “rich-get-richer” effect in which papers that have been cited more often in the past are cited at a higher rate in the future. The TVNLE plot in Fig. 5(b) qualitatively confirms this by showing a monotone effect of the covariate throughout the observation period (although the increase is somewhat steeper in the middle and flatter for the earlier and later time points).

In summary, our empirical analysis suggests that in relevant hyperevent networks we can find effects that are approximately monotone and constant over time (paper citation popularity), time-varying but almost monotone (cite paper and its references), non-monotone but mostly constant over time (difference in prior papers), or jointly time-varying and non-monotone (self citation).

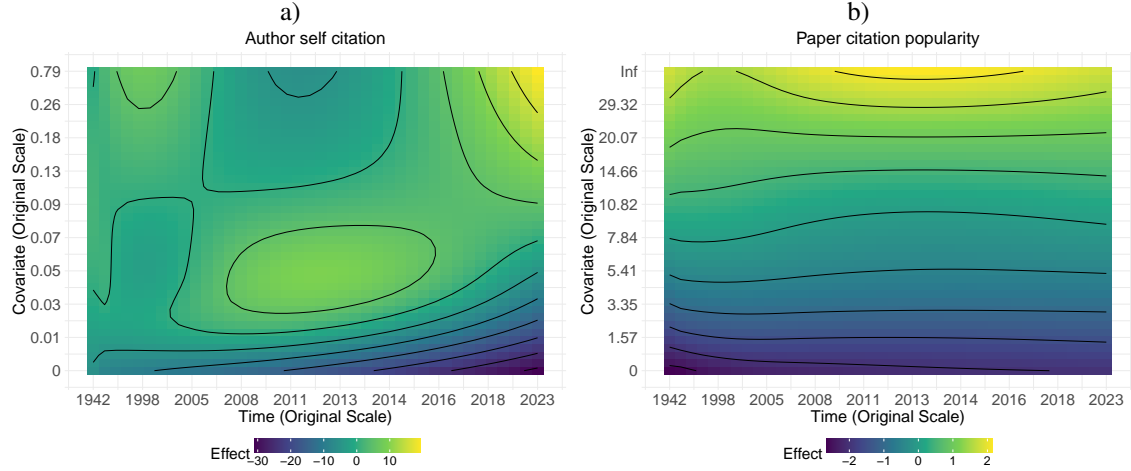


Figure 5: **Estimated TVLE of Author Self-Citation and Paper Citation Popularity.** a) Estimated TVNLE (log-hazard contribution) of Author self-citation. The plot suggests a monotone effect at the beginning and end of the observation period. However, between 2008 and 2016, the effect is non-monotonic: it first increases with the covariate value, then decreases. In this case, using a TVNLE is essential, as the effect changes qualitatively over time and varies with the covariate. b) Estimated TVNLE (log-hazard contribution) of Paper Citation Popularity. The plot indicates a monotone effect that is approximately constant over time. For larger covariate values, the effect slightly varies across the time range, suggesting some mild time-dependence, but still being monotonically increasing.

5 Discussion

In this paper, we have demonstrated how tensor product smooths can be used to model time-varying non-linear effects dynamics within the framework of relational hyperevent models. We applied this approach to study the dynamics of citation and impact. Particularly in the context of the time-sensitive relational event process, this is a valuable addition in the network modeling toolbox.

Strictly related to that, joint time-varying non-linear effects represent a powerful tool to discover patterns that not only may be non-linear but also non-monotonic. Indeed, when assuming linearity of the effect, we implicitly assume that either the effect is always increasing or always decreasing. This may not always be the case. As shown in the empirical application presented in this paper, there are situations where the effect of a covariate reaches a maximum or minimum and then reverses its trend. For example, certain factors may encourage the occurrence of events up to a certain threshold, but beyond that point, they may become counterproductive. A concrete case is author self-citation: citing a certain share of one's own work seems natural and in fact may be nearly unavoidable, as the own prior work may be among the most related to a new publication. However, excessive self-citation could be perceived negatively by the research community and would not well connect the new work to that of others. These aspects would not be possible to capture in a purely linear setting.

We showed how the dynamics related to a specific driver of the hyperevent data-generating process can be represented using two-dimensional heatmaps. What is relevant about this approach is that each heatmap reflects the most appropriate functional form according to the data. As for time-varying and non-linear effects, when dealing with a joint time-varying non-linear effect, we let the contribution of each covariate take a data-driven shape. This increased flexibility comes at a computational cost. For each covariate, we need to estimate $L \times Q$, where Q is the basis dimension related to non-linearity of the covariate and L is the basis dimension related to time. In the linear approach, for one covariate, we just need a single slope parameter. When dealing with many covariates, as in high-dimensional settings, this can pose a significant challenge — especially when estimation relies on inverting the Hessian matrix. It would therefore be important to adapt stochastic gradient descent techniques, such as those proposed in Filippi-Mazzola and Wit [2024b], to relational hyperevent models and, in particular, to these types of flexible effect specifications.

Whereas in this paper we focused on relational hyperevent models, also in the usual REM context, when dealing with dyadic relational events, one could consider incorporating this more flexible type of effect. Modeling and inference guidelines would remain largely the same.

6 Acknowledgments

This work was supported by the Swiss National Science Foundation [grant 192549]; and the Deutsche Forschungsgemeinschaft (DFG) [Project No. 321869138].

7 Declaration of interest

None.

8 Author contributions

MB: Conceptualization, Methodology, Software, Formal analysis, Writing - Original Draft; **JL**: Conceptualization, Methodology, Software, Resources, Data Curation, Writing - Review & Editing; **EW**: Conceptualization, Methodology, Writing - Review & Editing, Supervision;

References

- Viviana Amati, Alessandro Lomi, and Tom AB Snijders. A goodness of fit framework for relational event models. *Journal of the Royal Statistical Society Series A: Statistics in Society*, page qnae016, 2024. doi: 10.1093/jrsssa/qnae016.
- Giuseppe Arena, Joris Mulder, and Roger Th AJ Leenders. How fast do we forget our past social interactions? understanding memory retention with parametric decays in relational event models. *Network Science*, 11(2):267–294, 2023. doi: 10.1017/nws.2023.5.
- Julia Atienza-Barthelemy, Juan C Losada, and Rosa M Benito. Modeling information diffusion on social media: The role of the saturation effect. *Mathematics*, 13(6):963, 2025. doi: 10.3390/math13060963.
- Verena Bauer, Dietmar Harhoff, and Göran Kauermann. A smooth dynamic network model for patent collaboration data. *ASTA advances in statistical analysis*, 106(1):97–116, 2022. doi: 10.1007/s10182-021-00393-w.
- Austin R Benson, Ravi Kumar, and Andrew Tomkins. Sequences of sets. In *Proceedings of the 24th ACM SIGKDD international conference on knowledge discovery & data mining*, pages 1148–1157, 2018. doi: 10.1145/3219819.3220100.
- Claude Berge. *Hypergraphs: combinatorics of finite sets*. North-Holland, 1989.
- Federica Bianchi and Alessandro Lomi. From ties to events in the analysis of interorganizational exchange relations. *Organizational research methods*, 26(3):524–565, 2023. doi: 10.1177/10944281211058469.
- Federica Bianchi, Edoardo Filippi-Mazzola, Alessandro Lomi, and Ernst C Wit. Relational event modeling. *Annual Review of Statistics and Its Application*, 11, 2024. doi: 10.1146/annurev-statistics-040722-060248.
- Martina Boschi and Ernst-Jan Camiel Wit. Goodness of fit of relational event models. *arXiv preprint arXiv:2407.08599*, 2024. doi: 10.48550/arXiv.2407.08599.
- Martina Boschi, Rūta Juozaitienė, and Ernst C Wit. Mixed additive modelling of global alien species co-invasions of plants and insects. *Journal of the Royal Statistical Society Series C: Applied Statistics*, page qlaf034, 2025. doi: 10.1093/jrsssc/qlaf034.
- David Bright, Jürgen Lerner, and Giovanni Radhitio Putra Sadewo. Examining co-offending and re-offending across crime categories using relational hyperevent models. *Journal of Criminology*, 0(0):26338076241272864, 2024. doi: 10.1177/26338076241272864. URL <https://doi.org/10.1177/26338076241272864>.
- Katharina Burgdorf, Mark Wittek, and Jürgen Lerner. Communities of style: Artistic transformation and social cohesion in hollywood, 1930 to 1999. *Socius*, 10:23780231241257334, 2024. doi: 10.1177/23780231241257334. URL <https://doi.org/10.1177/23780231241257334>.
- Carter T Butts. A relational event framework for social action. *Sociological methodology*, 38(1):155–200, 2008. doi: 10.1111/j.1467-9531.2008.00203.x.
- Edoardo Filippi-Mazzola and Ernst C Wit. Modeling non-linear effects with neural networks in relational event models. *Social Networks*, 79:25–33, 2024a. doi: 10.1016/j.socnet.2024.05.004.
- Edoardo Filippi-Mazzola and Ernst C Wit. A stochastic gradient relational event additive model for modelling us patent citations from 1976 to 2022. *Journal of the Royal Statistical Society Series C: Applied Statistics*, page qlae023, 2024b. doi: 10.1093/jrsssc/qlae023.
- Edoardo Filippi-Mazzola, Federica Bianchi, and Ernst C Wit. Analyzing non-linear network effects in the european interbank market. In *2024 11th IEEE Swiss Conference on Data Science (SDS)*, pages 16–22. IEEE, 2024. doi: 10.1109/SDS60720.2024.00010.
- Joachim Hartung, Guido Knapp, and Bimal K Sinha. *Statistical meta-analysis with applications*. John Wiley & Sons, 2011. doi: 10.1002/9780470386347.
- Jarno Hoekman, Koen Frenken, and Robert JW Tijssen. Research collaboration at a distance: Changing spatial patterns of scientific collaboration within europe. *Research policy*, 39(5):662–673, 2010. doi: 10.1016/j.respol.2010.01.012.
- Rūta Juozaitienė and Ernst C Wit. Nodal heterogeneity can induce ghost triadic effects in relational event models. *Psychometrika*, 89(1):151–171, 2024. doi: 10.1007/s11336-024-09952-x.
- Rūta Juozaitienė, Hanno Seebens, Guillaume Latombe, Franz Essl, and Ernst C Wit. Analysing ecological dynamics with relational event models: The case of biological invasions. *Diversity and Distributions*, 29(10):1208–1225, 2023. doi: 10.1111/ddi.13752.
- Rūta Juozaitienė and Ernst C Wit. It's about time: Revisiting reciprocity and triadicity in relational event analysis. *Journal of the Royal Statistical Society Series A: Statistics in Society*, page qnae132, 2024. doi: 10.1093/jrsssa/qnae132.

- Marek Kwiek. What large-scale publication and citation data tell us about international research collaboration in europe: Changing national patterns in global contexts. *Studies in Higher Education*, 46(12):2629–2649, 2021. doi: 10.1080/03075079.2020.1749254.
- Renaud Lambiotte and Naoki Masuda. *A Guide to Temporal Networks*, volume 4. World Scientific, 2016.
- Geon Lee and Kijung Shin. Temporal hypergraph motifs. *Knowledge and Information Systems*, 65(4):1549–1586, 2023. doi: 10.1007/s10115-023-01837-2.
- Jürgen Lerner and Alessandro Lomi. Relational hyperevent models for polyadic interaction networks. *Journal of the Royal Statistical Society Series A: Statistics in Society*, 186(3):577–600, 2023. doi: 10.1093/jrsssa/qnac012.
- Jürgen Lerner, Margit Bussmann, Tom AB Snijders, and Ulrik Brandes. Modeling frequency and type of interaction in event networks. *Corvinus journal of sociology and social policy*, 4(1):3–32, 2013. doi: 10.14267/cjssp.2013.01.01.
- Jürgen Lerner, Marian-Gabriel Hâncean, and Alessandro Lomi. Relational hyperevent models for the coevolution of coauthoring and citation networks. *Journal of the Royal Statistical Society Series A: Statistics in Society*, 188(2): 583–607, 2025. doi: 10.1093/jrsssa/qnae068.
- Jürgen Lerner and Alessandro Lomi. Reliability of relational event model estimates under sampling: How to fit a relational event model to 360 million dyadic events. *Network Science*, 8(1):97–135, 2020. doi: 10.1017/nws.2019.57.
- Jürgen Lerner, Alessandro Lomi, John Mowbray, Neil Rollings, and Mark Tranmer. Dynamic network analysis of contact diaries. *Social Networks*, 66:224–236, 2021. ISSN 0378-8733. doi: <https://doi.org/10.1016/j.socnet.2021.04.001>. URL <https://www.sciencedirect.com/science/article/pii/S0378873321000277>.
- Ashwin Paranjape, Austin R Benson, and Jure Leskovec. Motifs in temporal networks. In *Proceedings of the tenth ACM international conference on web search and data mining*, pages 601–610, 2017. doi: 10.1145/3018661.3018731.
- Patrick O Perry and Patrick J Wolfe. Point process modelling for directed interaction networks. *Journal of the Royal Statistical Society Series B: Statistical Methodology*, 75(5):821–849, 2013. doi: 10.1111/rssb.12013.
- Stephen B Seidman. Structures induced by collections of subsets: A hypergraph approach. *Mathematical Social Sciences*, 1(4):381–396, 1981. doi: 10.1016/0165-4896(81)90016-0.
- Jie Tang, Jing Zhang, Limin Yao, Juanzi Li, Li Zhang, and Zhong Su. Arnetminer: extraction and mining of academic social networks. In *Proceedings of the 14th ACM SIGKDD international conference on Knowledge discovery and data mining*, pages 990–998, 2008. doi: 10.1145/1401890.1402008.
- Jingjing Wang, Yanhao Wang, Wenjun Jiang, Yuchen Li, and Kian-Lee Tan. Efficient sampling algorithms for approximate temporal motif counting. In *Proceedings of the 29th ACM international conference on information & knowledge management*, pages 1505–1514, 2020.
- Stanley Wasserman. Social network analysis: Methods and applications. *The Press Syndicate of the University of Cambridge*, 1994. doi: 10.1017/CBO9780511815478.
- Simon N. Wood. Thin Plate Regression Splines. *Journal of the Royal Statistical Society Series B: Statistical Methodology*, 65(1):95–114, January 2003. ISSN 1369-7412. doi: 10.1111/1467-9868.00374. URL <https://doi.org/10.1111/1467-9868.00374>. _eprint: https://academic.oup.com/rssb/article-pdf/65/1/95/49799823/jrssb_65_1_95.pdf.
- Simon N Wood. *Generalized additive models: an introduction with R*. Chapman and Hall/CRC, 2017. doi: 10.1201/9781315370279.
- Na Zou and Jing Li and. Modeling and change detection of dynamic network data by a network state space model. *IIE Transactions*, 49(1):45–57, 2017. doi: 10.1080/0740817X.2016.1198065. URL <https://doi.org/10.1080/0740817X.2016.1198065>.